NAMT

96-024

On the Radius-Edge Condition in the Control Volume
Method

Gary L. Miller
School of Computer Science,
Carnegie Mellon Univ.

Dafna Talmor
School of Computer Science,
Carnegie Mellon Univ.

Shang-Hua Teng
Dept. of Computer Science, U
niversity of Minnesota

Noel Walkington
Dept. of Mathematical Sciences,
Carnegie Mellon Univ.

Research Report No. 96-NA-024

December 1996

UMAT
HG0 .O94

On the Radius–Edge Condition in the Control Volume Method[*]

Gary L. Miller[†], Dafna Talmor[*] , Shang-Hua Teng[‡] AND Noel Walkington[§]

Abstract. In this paper we show that the control volume algorithm for the solution of Poisson's equation in three dimensions will converge when the mesh contains very flat tetrahedra (slivers). These tetrahedra are characterized by the fact that they have modest ratios of diameter to shortest edge, but large circum to inscribed sphere radius ratios, so may have poor interpolation properties. Elimination of slivers is a notoriously difficult problem for automatic mesh generation algorithms. We also show that a discrete Poincaré inequality will continue to hold in the presence of slivers.

1. Introduction. We consider covolume approximations of Poisson's equation on a three dimensional domain. It is shown that the control volume algorithm will converge on Delaunay meshes that contain "slivers"; that is, flat tetrahedra whose vertices are approximately equi–spaced around the euqator of a sphere (see Figure 1). This result is was rather unexpected, since the classical finite element algorithm may fail to converge when such elements are present.

Classical finite element theory shows that the finite element solution is the best approximation of the solution in the $H_0^1(\Omega)$ norm[1], so clearly the control volume algorithm can't converge in this norm if the finite element solution doesn't. Instead we show that the control volume scheme converges in a discrete $H_0^1(\Omega)$ norm ($\|.\|_W$ below), and like the finite element algorithm, the control volume algorithm gives the best projection with respect to this norm. Numerical experiments indicate that the finite element method fails to converge in either norm. We note that in two dimensions the two norms coincide, so this dichotomy is truly a three dimensional phenomenon. Since the discrete norm used with the control volume algorithm changes with the mesh, it is natural to ask if convergence can be established in any of the standard norms. We answer this in the affirmative by establishing a discrete Poincaré inequality which will imply convergence of the control volume method in $L^2(\Omega)$.

These results evolved from our work on mesh generation algorithms [6, 7] and an attempt to resolve the problems slivers present in approximation theory. The mesh generation algorithms we developed produce tetrahedra having bounded ratios of circum radius to minimum edge length (radius edge ratio), while traditional interpolation theory requires each tetrahedra to have the classical aspect ratio of circum to inscribed sphere radii bounded. Slivers, which have a radius edge ratio near unity and arbitrarily small volume, show that a bounded radius edge aspect ratio is a weaker condition than the classical aspect ratio in three dimensions. (Of course they're equivalent in two dimensions.) While a bound on the classical aspect ratio is sufficient for optimal interpolation, it is not necessary. Babuška and Aziz [1] showed that right triangles in two dimensions, and their analogues in three dimensions, will exhibit optimal interpolation even if they have arbitrarily small volume. In two dimensions this leads to a the very simple geometric requirement that "the maximum angle within any triangle be bounded away from π"; however, no simple geometric restriction is known for tetrahedra. Upon

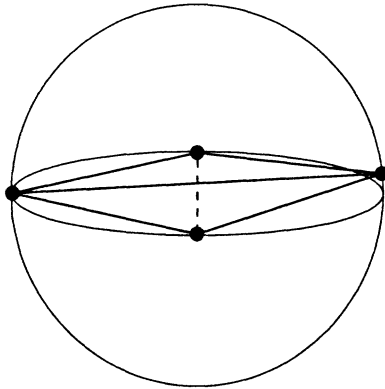[1] $\|u\|_{H_0^1(\Omega)}^2 = \int_\Omega |\nabla u|^2$

FIG. 1. *Sliver and circum sphere.*

discovering that the covolume scheme converges in the presence of slivers, it is natural to ask if they too exhibit optimal interpolation properties. Folk lore indicates that they do not, and this is substantiated by the numerical example in Section 3.

In order to put the geometric assumptions in context, Section 2 reviews the essential features of the mesh generation algorithm developed in [7]. As indicated above, this algorithm does guarantees a bound on the radius edge aspect ratio. The proof of convergence for Poisson's equation under the bounded radius edge ratio assumption is presented Section 3 along with an example which highlights the differences between the covolume and finite element schemes. In Section 4 a discrete Poincaré inequality is established which provides one method of passing from mesh dependent norms to the $L^2(\Omega)$ norm.

2. Sphere Packings and Mesh Generation. Mesh generation has a long history; however, rigorous analysis of the algorithms and the meshes they produce is a recent development. Bern Epstein and Gilbert [2] were the first to establish optimality of the the quad–tree algorithm for the generation of two dimensional meshes. By optimal we mean that bounds on the aspect ratio of each triangle can be established a–priori and that the number of triangles produced is within a constant of the minimum possible. Unfortunately the constant for the quad–tree algorithm appears to be rather large, so that this, and it's three dimensional counterpart [8], is not a particularly practical approach. An optimal two dimensional algorithm that appears to work very well in practice was given by Ruppert [10]. This algorithm extended an idea of Chew [3], and uses the Voronoi/Delaunay constructions. Ruppert's algorithm doesn't extend immediately to three dimensions since it may produce "slivers", that is, very flat tetrahedra whose edge lengths are comparable with the circum sphere radius (see Figure 1). These flat tetrahedra are difficult to eliminate, and plague all three dimensional mesh generation algorithms. In Section 3 we establish the rather unexpected result that these slivers do not degrade control volume approximations of Poisson's equation, and in this situation extensions of Ruppert's algorithm can be used to produce meshes that are "provable good for control volume approximations". The remainder of this section introduces the basic geometric properties needed for the analysis in Sections 3 and 4.

Below we consider meshes generated as the Delaunay diagrams of a set of points $X = \{x_i\} \subset \bar{\Omega} \subset \Re^d$ (we are particularly interested in three dimensions where $d = 3$). Recall that the Voronoi diagram is the collection of polytopes $\{V_i\}$ where V_i is the subset of points in Ω closer to x_i than to any other point in the set X. The Delaunay triangulation is then constructed by joining points in X that share a common Voronoi face. This construction is well known in computational geometry [4], and there are efficient algorithms for implementing it in any number of dimensions, and will generate a graded mesh according to the distribution of the points in X.

2

The meshes we consider below assume that the triangulation satisfies the following weakened aspect ratio condition:

DEFINITION 2.1 (BOUNDED RADIUS-EDGE RATIO). *The* **radius-edge ratio** *of a triangulation in three dimensions is the maximum ratio of circumscribed sphere radius to smallest edge length of any tetrahedra.*

We briefly sketch one technique for generating a vertex sets whose Delaunay triangulations have bounded radius–edge ratios. We assume that we're given a function $\rho : \Omega \to \Re^+$ which locally specifies the desired density of mesh points in Ω.

DEFINITION 2.2. *A collection of points $X = \{x_1, x_2, \ldots, x_N\} \subset \Omega$ is a ρ-packing if x_i, $x_j \in X$ implies $[\rho(x_i) + \rho(x_j)]/2 \le |x_i - x_j|$ where $|.|$ denotes Euclidean distance.*

A simple algorithm for the construction of a maximal ρ-packing is to initialize X to be the empty set and to randomly select a point from $x \in \Omega$ and add it to X if the sphere of radius $\rho(x)$ centered at x doesn't meet the analogous spheres of any point already in X. Upon termination, X will be a maximal ρ-packing. The following lemma concerning the Voronoi/Delaunay diagram for X is elementary.

LEMMA 2.3. *Let $\rho : \Omega \to \Re^+$ be Lipschitz[2] with $|\rho|_{Lip} < 2$ and let X be a maximal ρ-packing. If v is the center of a Delaunay ball (i.e. the circumsphere of a tetrahedra) of radius r in the Voronoi/Delaunay triangulation of X then $\rho(v) \ge (1 - |\rho|_{Lip}/2)r$.*

This lemma and the following corollary are proved in [6, 7], and provide a wealth of geometric information about such meshes.

COROLLARY 2.4. *Let $\alpha = |\rho|_{Lip} < 2/3$, then*

- *If v and r are as in the lemma and $x \in B_r(v)$, the ball or radius r centered at v, then $\rho(x) \ge (1 - 3\alpha/2)r$.*
- *The radius–edge ratio of the Delaunay triangulation of X is bounded by $1/(1 - 3\alpha/2)$.*
- *If V is a Voronoi polytope centered at $x \in X$, the ratio of circum radius of V to inscribed radius of V (with center x) is bounded by $(2 + \alpha)/(1 - 3\alpha/2)$.*
- *If x, $y \in X$ and $p \in \overline{xy}$ (an edge in the Delaunay diagram) then*

$$\rho(p) \ge \frac{1 - 3\alpha/2}{2 + \alpha}\rho(x).$$

- *For any Voronoi region V*

$$\frac{\max_V \rho}{\min_V \rho} \le \frac{(2 + \alpha)(2 + 3\alpha/2)}{(1 - 3\alpha/2)^2}.$$

The development of ideas sketched in this section began with a spacing function ρ and lead to a mesh with a bounded radius–edge ratio. It is also possible to do the converse. Theorem 4.4 in Section 4 shows that a Delaunay mesh having bounded radius edge ratio determines a Lipschitz spacing function ρ satisfying the properties stated in the corollary.

3. Co–Volume Approximations.

3.1. Notation. Let $\Omega \subset \Re^3$ be a bounded open set, and consider the problem of finding $u : \Omega \to \Re$ such that

$$-\Delta u = f, \quad \text{in } \Omega, \quad u|_{\partial\Omega} = g.$$

To approximate u, Ω is first triangulated; the triangulation being the Delaunay triangulation of a set of points $\{x_i\}$. We denote the length of the Delaunay edge joining vertex x_i to x_j by h_{ij}, and denote

---

[2] Recall that ρ is Lipschitz with constant $|\rho|_{Lip} \le \alpha$ if $|\rho(x) - \rho(y)| \le \alpha|x - y|$ for all x and y.

3

by V_i the Voronoi region associated with node x_i. To minimize technical details we assume that the mesh accommodates the boundary in a fashion guaranteeing that the Voronoi V_i corresponding to an interior vertex x_i lies entirely within Ω. Each edge $\overline{x_i x_j}$ of the Delaunay mesh can be associated with a face common to V_i and V_j which we denote by A_{ij}.

Following MacNeal [5] discrete approximations of u are constructed by integrating the equation for u over each Voronoi corresponding to an interior vertex:

$$
\begin{aligned}
\int_{V_i} f &= \int_{V_i} -\Delta u = \int_{\partial V_i} -\frac{\partial u}{\partial n} \\
&= \sum_{j \in \mathcal{N}_i} \int_{A_{ij}} -\frac{\partial u}{\partial n} \simeq \sum_{j \in \mathcal{N}_i} |A_{ij}| \frac{u_i - u_j}{h_{ij}}
\end{aligned}
$$

In the above, $\mathcal{N}_i$ is the index set of the nodes connected to x_i by an edge, u_i is an approximation of $u(x_i)$, and $|A_{ij}|$ denotes the surface area of the Voronoi face A_{ij}. Letting f_i denote the average value of f over V_i this scheme becomes

$$
\sum_{j \in \mathcal{N}_i} |A_{ij}| \frac{u_i - u_j}{h_{ij}} = |V_i| f_i, \qquad \forall \; x_i \text{ interior},
$$

and $u_i = g(x_i)$ for the boundary vertices.

3.2. Orthogonality and Convergence. Nicolaides [9] introduced the following elegant analysis of the above scheme. First, note that the exact solution u of the equation satisfies

$$
\begin{aligned}
\int_{V_i} f = \int_{V_i} -\Delta u &= \int_{\partial V_i} \frac{\partial u}{\partial n} = \sum_{j \in \mathcal{N}_i} \int_{A_{ij}} -\frac{\partial u}{\partial n} \\
|V_i| f_i &= \sum_{j \in \mathcal{N}_i} |A_{ij}| U_{ij}^{(2)}
\end{aligned}
$$

Where $U_{ij}^{(2)}$ is the average value of the flux $-\partial u/\partial n$ on the face A_{ij}. Upon subtracting this from the equation satisfied by the discrete solution we obtain

$$
0 = \sum_{j \in \mathcal{N}_i} |A_{ij}| (U_{ij} - U_{ij}^{(2)})
$$

where $U_{ij} = (u_i - u_j)/h_{ij}$ is the discrete flux.

The second step is to consider an arbitrary set of nodal values $\{v_i\}$ that vanish on the boundary. Multiplying the above equation by v_i and summing over all of the interior nodes gives

$$
\begin{aligned}
0 &= \sum_{i} \sum_{j \in \mathcal{N}_i} |A_{ij}| (U_{ij} - U_{ij}^{(2)}) v_i \\
&= \sum_{\overline{x_i x_j}} |A_{ij}| (U_{ij} - U_{ij}^{(2)})(v_i - v_j) \\
&= \sum_{\overline{x_i x_j}} |A_{ij}| h_{ij} (U_{ij} - U_{ij}^{(2)}) V_{ij}
\end{aligned}
$$

where $\sum_{\overline{x_i x_j}}$ indicates summation over the non-boundary edges, and $V_{ij} = (v_i - v_j)/h_{ij}$. Defining the inner product $[.,.]_W$ on quantities defined upon the non-boundary edges by

$$
[U, V]_W = \sum_{\overline{x_i x_j}} |A_{ij}| h_{ij} \, U_{ij} V_{ij}
$$

4

we may write $[U - U^{(2)}, V]_W = 0$ where it is understood that U is the discrete flux given by the co-volume scheme and the discrete flux V must be the discrete gradient of a piecewise linear function v vanishing on the boundary, i.e. $V_{ij} = (v_i - v_j)/h_{ij}$.

An error estimate can now follows by recognizing that the above orthogonality relationship states that the co-volume approximation is the best projection of the flux $U^{(2)}$ onto the space of fluxes generated by discrete functions vanishing on the boundary. In particular, if we let $U_{ij}^{(1)} = (u(x_i) - u(x_j))/h_{ij}$ be the flux determined by the interpolant of the exact solution we obtain

$$\|U - U^{(1)}\|_W \leq \|U^{(2)} - U^{(1)}\|_W.$$

The following theorem characterizes the size of the approximation error on the right hand side of this expression.

THEOREM 3.1. Let[3] $u \in H^2(\Omega)$ and $U_{ij}^{(1)} = (u(x_i) - u(x_j))/h_{ij}$ be the approximation of the flux $U_{ij}^{(2)} = (-1/A_{ij}) \int_{A_{ij}} \partial u / \partial n$, then

$$\|U^{(2)} - U^{(1)}\|_W \leq \frac{1}{2} \max_{x_i, x_j} \left[1 + 4(r_{ij}/h_{ij})^2 h_{ij} \right] \|D^2 u\|_{L^2(\Omega)},$$

where r_{ij} is maximum radius of a control volume having A_{ij} as a face. In particular, if the mesh has a bounded radius–edge ratio the error in the co–volume scheme is given bounded by

$$\|U - U^{(1)}\|_W \leq \frac{1}{2}(1 + 4B^2)\|D^2 u\|_{L^2(\Omega)} h,$$

where $h = \max_{\overline{x_i x_j}} h_{ij}$.

Proof. Let us write

$$\|U^{(2)} - U^{(1)}\|_W^2 = \sum_{x_i, x_j} |A_{ij}| h_{ij} \, \mu_{ij}(u)^2$$

where

$$\mu_{ij}(u) = \frac{-1}{A_{ij}} \int_{A_{ij}} \frac{\partial u}{\partial n} - \frac{u(x_i) - u(x_j)}{h_{ij}}$$

We explicitly compute the term $\mu_{ij}(u)$ for a generic edge h_{ij}. It is convenient to put the origin at the middle of h_{ij} and let h_{ij} lie in the z–axis so that A_{ij} lies in the plane $z = 0$, and for definiteness let h_{ij} point from x_i to x_j up the z–axis. Next, let K_{ij}^+ be the cone with vertex x_j and base A_{ij} and K_{ij}^- be the cone with vertex x_i and base A_{ij}, and note that cones corresponding to different Voronoi faces A_{ij} are disjoint, and the union of all such cones is the union of the Voronoi regions V_i corresponding to internal vertices x_i (see Figure 2).

For the calculations below we drop the subscript ij, so that $h = h_{ij}$, $A = A_{ij}$ etc. The cone K^+ may be parameterized by

$$x = (1 - 2\eta/h)\xi_1, \qquad y = (1 - 2\eta/h)\xi_2, \qquad z = \eta,$$

$(\xi_1, \xi_2) \in A$, $0 \leq \eta \leq h/2$. Note that

$$\int_{K^+} u = \int_A \int_0^{h/2} u(\xi_1, \xi_2, \eta)\,(1 - 2\eta/h)^2 \, d\eta \, d\xi$$

---

[3] $H^2(\Omega)$ is the set of functions in $L^2(\Omega)$ having all second derivatives in $L^2(\Omega)$
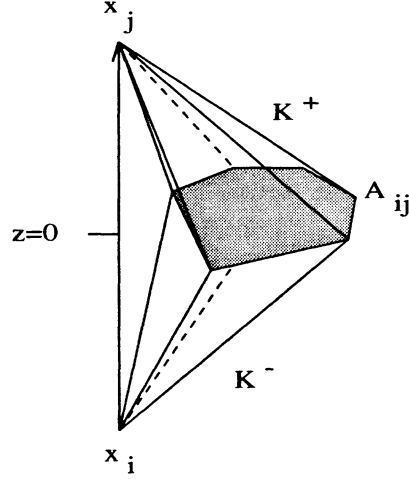
FIG. 2. *Cones constructed in Theorem 3.1.*

where $d\xi = d\xi_1\, d\xi_2$. Also

$$\frac{\partial u}{\partial \eta} = -2\frac{\xi_1}{h}\frac{\partial u}{\partial x} - 2\frac{\xi_2}{h}\frac{\partial u}{\partial y} + \frac{\partial u}{\partial z}$$

$$\frac{\partial^2 u}{\partial \eta^2} = (-2\xi_1/h, -2\xi_2/h, 1)[D_x^2 u](-2\xi_1/h, -2\xi_2/h, 1)^T, \qquad \left|\frac{\partial^2 u}{\partial \eta^2}\right| \le \left[1 + 4(\xi_1^2 + \xi_2^2)/h^2\right]|D^2 u|.$$

We now compute

$$
\begin{aligned}
\int_{K^+} \frac{1}{1 - 2(\eta/h)}\frac{\partial^2 u}{\partial \eta^2} &= \int_A \int_0^{h/2} \frac{\partial^2 u}{\partial \eta^2}(1 - 2\eta/h)\, d\eta\, d\xi \\
&= \int_A \left\{ \frac{\partial u}{\partial \eta}(1 - 2\eta/h)|_0^{h/2} + \frac{2}{h}\int_0^{h/2}\frac{\partial u}{\partial \eta}\, d\eta \right\}\, d\xi \\
&= \int_A \left\{ -\frac{\partial u}{\partial \eta}(\xi_1, \xi_2, 0^+) + \frac{2}{h}(u(x_j) - u(\xi_1, \xi_2, 0^+)) \right\}\, d\xi \\
&= \int_A \left\{ -\frac{\partial u}{\partial \eta}(\xi_1, \xi_2, 0^+) - 2u(\xi_1, \xi_2, 0^+)/h \right\}\, d\xi + 2|A|u(x_j)/h.
\end{aligned}
$$

Repeat this computation for the bottom cone using the parameterization

$$x = (1 + 2\eta/h)\xi_1, \qquad y = (1 + 2\eta/h)\xi_2, \qquad z = \eta,$$

$(\xi_1, \xi_2) \in A$, $-h/2 \le \eta \le 0$, to obtain

$$\int_{K^-} \frac{1}{1 + 2(\eta/h)}\frac{\partial^2 u}{\partial \eta^2} = \int_A \left\{ \frac{\partial u}{\partial \eta}(\xi_1, \xi_2, 0^-) - 2u(\xi_1, \xi_2, 0^-)/h \right\}\, d\xi + 2|A|u(x_i)/h.$$

Continuity of u guarantees that $u(.,0^+) = u(.,0^-)$ so that

$$
\begin{aligned}
\int_{K^+} \frac{1}{1 + 2(\eta/h)}&\frac{\partial^2 u}{\partial \eta^2} - \int_{K^-} \frac{1}{1 - 2(\eta/h)}\frac{\partial^2 u}{\partial \eta^2} \\
&= -\int_A \left\{ \frac{\partial u}{\partial \eta}(\xi_1, \xi_2, 0^-) + \frac{\partial u}{\partial \eta}(\xi_1, \xi_2, 0^+) \right\}\, d\xi - 2|A|\frac{u(x_i) - u(x_j)}{h}.
\end{aligned}
$$

6

Note that $\partial u/\partial\eta = 2(\xi_1/h)\partial u/\partial x + 2(\xi_2/h)\partial u/\partial y + \partial u/\partial z$, in K^- so that

$$\int_{K^+}\frac{1}{1+2\eta/h}\frac{\partial^2 u}{\partial\eta^2} - \int_{K^-}\frac{1}{1-2\eta/h}\frac{\partial^2 u}{\partial\eta^2} = 2\int_A -\frac{\partial u}{\partial z}\Big|_{z=0} - 2|A|\frac{u(x_i)-u(x_j)}{h}$$
$$= 2|A|\,\mu(u).$$

It remains to bound the terms involving the second derivatives.

$$\left|\int_{K^+}\frac{1}{1-2(\eta/h)}\frac{\partial^2 u}{\partial\eta^2}\right| \leq \left|\int_{K^+}\frac{1+4(\xi_1^2+\xi_2^2)/h^2}{1-2(\eta/h)}|D^2 u|\right|$$
$$\leq \left\|\frac{1+4(\xi_1^2+\xi_2^2)/h^2}{1-2(\eta/h)}\right\|_{L^2(K^+)}\|D^2 u\|_{L^2(K^+)}$$
$$\leq (1/2)\sqrt{|A|h}\left[1+4(r/h)^2\right]\|D^2 u\|_{L^2(K^+)},$$

where $r^2 = \max_{(\xi_1,\xi_2)\in A}(\xi_1^2+\xi_2^2)$. A similar computation for the lower cone gives

$$\mu(u) \leq \frac{1}{2}\sqrt{\frac{h}{|A|}}\left[1+4(r/h)^2\right]\|D^2 u\|_{L^2(K^++\cup K^-)}.$$

Putting it all together:

$$\|U-U^{(1)}\|_W \leq \|U^{(2)}-U^{(1)}\|_W = \left(\sum_{x_i,x_j}|A_{ij}|h_{ij}\,\mu_{ij}(u)^2\right)^{1/2}$$
$$\leq (1/2)\max_{x_i,x_j}\left[(1+4(r_{ij}/h_{ij})^2)h_{ij}\right]\left(\sum_{x_i,x_j}\|D^2 u\|^2_{L^2(K_{ij}^+\cup K_{ij}^-)}\right)^{1/2}$$
$$\leq (1/2)\max_{x_i,x_j}\left[(1+4(r_{ij}/h_{ij})^2)h_{ij}\right]\|D^2 u\|_{L^2(\Omega)}.$$

$\square$

3.3. Numerical Example. We illustrate the implications of our theorem with a numerical example. Meshes are constructed by dividing the unit cube into a uniform rectangular mesh, and then randomly perturbing the points by an amount ϵh. The Delaunay triangulation of such points will have multitudes of slivers on all of the vertical and horizontal planes where the points are almost co-circular. While the radius–edge ratio of these slivers will be near unity and their classical aspect ratio of diameter to inscribed sphere radius (d/r) will be very large when ϵ is small. Figure 3 tabulates the errors for the solution

$$u(x,y,z) = e^{\pi x}\cos(\pi y/\sqrt{2})\sin(\pi z/\sqrt{2})$$

of $-\Delta u = 0$ computed using the finite element and co-volume algorithms. It is clear that for h fixed the finite element errors increase as $\epsilon \to 0$ and the the co-volume error is independent of ϵ. Also, for ϵ fixed, the first order rate of convergence for the finite element solution in the $H_0^1(\Omega)$ norm is readily observable (the error decreases in proportion with h). The co–volume scheme achieves a higher rate of convergence (almost two) for this example since the mesh is almost uniform. On a uniform mesh the co–volume scheme is, in fact, second order accurate (this can readily be observed in the proof of Theorem 3.1).

| h | ϵ | d/r | FEM | | Co-Volume |
			$|u - u_h|_{H^1}$	$\|I_h u - u_h\|_W$	$\|I_h u - u_h\|_W$
1/4	0.01	1126	30.22479	7.696399	0.2425438
	0.001	11125	92.97309	8.692323	0.2411516
	0.0001	111296	291.6406	8.917005	0.2410718
1/8	0.01	26230	12.98964	4.344101	0.07616430
	0.001	166051	35.13775	6.865007	0.07531520
	0.0001	1621745	108.1435	7.525118	0.07538803
1/16	0.01	14194	6.023042	2.262189	0.02155074
	0.001	105551	15.48025	4.457009	0.02005826
	0.0001	1030956	45.91799	6.140328	0.02007369

FIG. 3. *Errors for control volume and finite element methods.*

4. Poincaré Inequality.

The Poincaré inequality states that for a bounded domain $\Omega \subset \mathfrak{R}^d$ there is a constant $C > 0$ such that $\|u\|_{L^2(\Omega)} \le C\|\nabla u\|_{L^2(\Omega)}$ for all sufficiently smooth functions $u : \Omega \to \mathfrak{R}$ vanishing on the boundary $\partial\Omega$. MacNeal [5] has shown that in two dimensions the W norm (defined in Section 3.2) is equal to the $H^1(\Omega)$ norm, in the sense that the piecewise linear extension, $\tilde{u}$, of u defined on the vertices of a triangulation satisfies $\|u\|_W^2 = \int_\Omega |\nabla \tilde{u}|^2$. The Poincaré inequality, $\int_\Omega u^2 \le C \int_\Omega |\nabla u|^2$ then implies that convergence of a discrete solution in the W norm implies convergence in $L^2(\Omega)$. In three dimensions the W norm is no longer equivalent to the $H^1(\Omega)$ norm, so convergence in $L^2(\Omega)$ doesn't follow directly from the Poincaré inequality. Below we establish a discrete Poincaré inequality for the W norm which establishes convergence in $L^2(\Omega)$ of the piecewise constant functions.

DEFINITION 4.1. *Given a real valued function u on the mesh vertices, the piecewise constant extension $\hat{u} : \Omega \to \mathfrak{R}$ is defined to be the function equal to u_i over the Voronoi cell V_i.*

The discrete $L^2(\Omega)$ norm of u is then interpreted to mean $\|\hat{u}\|_{L^2(\Omega)}^2 = \Sigma_i \int_{V_i} u_i^2$.

THEOREM 4.2 (DISCRETE POINCARÉ INEQUALITY). *Let u be a function defined on the vertices of a triangulation of the bounded domain $\Omega \subset \mathfrak{R}^d$ that vanishes on the boundary vertices. Then there exists $C > 0$ depending only upon Ω and the radius edge ratio of the mesh such that $\|u\|_{L^2(\Omega)} \le C\|u\|_W$.*

The theorem statement can be rewritten explicitly as:

$$\text{(1)} \qquad \sum_i |V_i| u_i^2 \le C \sum_{x_i x_j} \frac{|A_{ij}|}{h_{ij}} (u_i - u_j)^2$$

for all mesh functions vanishing on the boundary.

The meshes we consider are Delaunay diagrams, described by a set of vertices $X = \{x_i \cdots x_n\}$, a set of tetrahedra whose 1–skeleton is the edge set E and a set of Voronoi cells V. We define the following weighted graph associated with the mesh:

DEFINITION 4.3. *1) Let $\mathcal{G} = \mathcal{G}(X, E, V)$ denote the graph constructed from the Delaunay diagram $\mathcal{D} = (X, E, V)$ as follows:*

 X: the vertex set of the graph is identified with the vertex set of the Delaunay diagram.

 E: edges (i, j) in the graph correspond to interior Delaunay edges and have weight $k_{ij} = |A_{ij}|/h_{ij}$. Recall h_{ij} is the length of the Delaunay edge between two vertices, A_{ij} is the area of the Voronoi face shared by V_i and V_j.

 V: we assign a cell to each graph vertex.

8

2) The mass matrix M is a diagonal matrix containing the (truncated) Voronoi volumes on the diagonal. (Recall that Voronoi regions on the boundary may be infinite, so we only consider the part in Ω. We treat the areas used for computing the edge weights in a similar fashion. These terms are inconsequential since we only consider functions vanishing on the boundary.)

3) The Laplacian of the graph $\mathcal{G}$, denoted by K, is the matrix having off diagonal entries $K_{ij} = -|A_{ij}|/h_{ij} = -k_{ij}$ if (i,j) is an edge in $\mathcal{G}$ and zero otherwise and the diagonals are given by $K_{ii} = \sum_{j \neq i} k_{ij}$.

The discrete Poincaré inequality then states that the eigenvalues (on the space of vectors having zero boundary components) of the generalized eigenvalue problem $Ku = \lambda Mu$ are bounded below by a constant $c > 0$, or alternatively that there is a constant $c > 0$ such that $K - cM \geq 0$ (positive semi–definite).

4.1. Geometric Properties. The meshes we consider are Delaunay diagrams $\mathcal{D} = (X, E, V)$ where $X \subset \bar{\Omega} \subset \Re^d$. We assume the mesh tetrahedra are of bounded radius-edge ratio.

Delaunay diagrams of bounded radius-edge ratio have several important geometric properties. Below we recall some of these properties which were established in [6]. Recall that we denote the edge joining two vertices x_i and x_j by $\overline{x_i x_j}$ and the length of such an edge by h_{ij}, and that the set of vertices connected to vertex x_i by an edge is is denoted by $\mathcal{N}_i$. Also, we adopt the notation that C and c are positive constants which may differ from occurrence to occurrence. In general, c will be a lower bound and C an upper bound, and these constants only depend upon the mesh through the Lipschitz constant of the for the spacing function, ρ, appearing in the following theorem.

THEOREM 4.4. *Let $\mathcal{D} = (X, E, V)$ be a bounded radius-edge ratio Delaunay diagram. The following is true:*

A1) *There is a function $\rho : \Omega \to \Re^+$ with Lipschitz constant bounded by one and constants c, $C > 0$ such that for each internal vertex $x_i \in X$*

$$ch_{ij} \leq \rho(x) \leq Ch_{ij}, \qquad \forall j \in \mathcal{N}_i, \ x \in V_i$$

and for all edges $\overline{x_i x_j}$

$$ch_{ij} \leq \rho(x) \leq Ch_{ij}, \qquad \forall x \in \overline{x_i x_j}.$$

A2) *There is a constant $\theta > 0$ such that each region $V_i \cap \Omega$, where $V_i \in V$, contains a ball of radius $\theta\rho(x_i)$ centered at x_i, and is contained in a concentric ball of radius $\rho(x_i)/\theta$.*

A3) *There is a constant $C > 0$ such that each vertex $x_i \in X$ has at most C neighbors in the diagram, i.e. the associated graph has bounded degree.*

A4) *The area of the Voronoi face shared by vertices $x_i, x_j \in X$ is bounded from above by Ch_{ij}^{d-1}.*

The function ρ is referred to as the **spacing function** of the mesh, as it describes the typical distance between vertices. This function plays an important role in the proofs below as it captures many of the mesh properties.

Our arguments below are graph theoretic and don't use the fact that we're dealing with a Voronoi/Delaunay triangulation. Any decomposition of Ω into volumes V_i and edges connecting them that satisfy the geometric properties listed in Theorem 4.4 would suffice. We therefore generalize the notion of the bounded radius-edge ratio Delaunay diagram as follows:

DEFINITION 4.5 (WELL-SHAPED DIAGRAM). *A diagram $\mathcal{G} = (X, E, V)$ is a set of vertices X, and a set of cells V such that vertex $x_i \in V_i$, and the edge set E corresponds to the neighborhood structure of the cells. The diagram is* **well-shaped** *if properties A1-A4 hold.*

Notation: Since the edges of a well shaped diagram don't necessarily correspond to line segments in $\Re^d$ we will denote an edge connecting x_i, $x_j \in X$ by (i,j), and use the notation $\overline{x_i x_j}$ to suggest a line segment in $\Re^d$.

4.2. Comparison. Our proof of the discrete Poincaré inequality will parallel the proof of its continuous counterpart. The continuous proof considers a large cube Q containing Ω, and since all functions defined on Ω vanishing on the boundary can be extended by zero to all of Q, a Poincaré inequality on Q will imply a Poincaré inequality on Ω. We too will embed Ω into a large cube, and in this section we show that any two meshes on Ω and Q satisfying the geometric properties of Theorem 4.4 with the same spacing function ρ can be suitably compared. The next section will then show that for each spacing function there exists a canonical mesh on the cube for which the Poincaré inequality holds.

DEFINITION 4.6 (PATH EMBEDDING). *(1) The graph $\mathcal{G}_1 = (X^{(1)}, E^{(1)}, V^{(1)})$ is* **path embedded** *in $\mathcal{G}_2 = (X^{(2)}, E^{(2)}, V^{(2)})$ if there exists a function ϕ from $X^{(1)}$ to $X^{(2)}$ and a mapping p from the edges of $\mathcal{G}_1$ into paths in $\mathcal{G}_2$, such that for each edge (m,n) in $\mathcal{G}_1$, $p(m,n)$ is a path in $\mathcal{G}_2$ from $\phi(m)$ to $\phi(n)$.*

(2) The embedding has **bounded dilation** *if there is a constant $C_k > 0$ such that for every edge $(m,n) \in E^{(1)}$,*

$$\sum_{(i,j)\in p(m,n)} 1/k_{ij}^{(2)} \le C_k/k_{mn}^{(1)}$$

where $k_{mn}^{(1)}$ and $k_{ij}^{(2)}$ are the edge weights of $\mathcal{G}_1$ and $\mathcal{G}_2$ respectively (i.e. the conductivity of the path is comparable to the conductivity of the edge).

(3) The embedding has **bounded congestion** *if there is a constant $C_p > 0$ such that for each edge (i,j) in $\mathcal{G}_2$*

$$c_{ij} = \sum_{p(m,n)\ni(i,j)} 1 \le C_p$$

LEMMA 4.7. *Let (ϕ, p) be a path embedding of $\mathcal{G}_1$ into $\mathcal{G}_2$ with bounded dilation and congestion, and let u be a real valued function on the vertices of $\mathcal{G}_2$ and $u \circ \phi$ be the induced function on the vertices of $\mathcal{G}_1$. Then there is constant $C > 0$ such that*

$$(u \circ \phi)^T K^{(1)}(u \circ \phi) \le C u^T K^{(2)} u$$

Proof.

$$
\begin{aligned}
(u \circ \phi)^T K^{(1)}(u \circ \phi) &= \sum_{(m,n)} k_{mn}^{(1)}(u_{\phi(m)} - u_{\phi(n)})^2 \\
&= \sum_{(m,n)} k_{mn}^{(1)} \left(\sum_{(i,j)\in p(m,n)} (u_i - u_j) \right)^2 \\
&\le \sum_{(m,n)} k_{mn}^{(1)} \left(\sum_{(i,j)\in p(m,n)} 1/k_{ij}^{(2)} \right) \sum_{(i,j)\in p(m,n)} k_{ij}^{(2)}(u_i - u_j)^2 \\
&\le C_k \sum_{(m,n)} \sum_{(i,j)\in p(m,n)} k_{ij}^{(2)}(u_i - u_j)^2 \\
&\le C_k C_p \sum_{(i,j)} k_{ij}^{(2)}(u_i - u_j)^2 .
\end{aligned}
$$

10

□

Property A4 allows the edge weights A_{ij}/h_{ij} to be arbitrarily small. In particular, a sliver in a Delaunay diagram corresponds to a small weight. All the paths containing the "light" edge will have small conductivity. The following lemma states that this situation is not generic, and that each edge can be replaced by a path of high conductivity, which will be used for the construction of suitable path embeddings.

We plan to embed a cube Q into Ω and need a way of extending functions on Ω that vanish on the boundary to all of Q. A convenient way of doing this is to add a "super" node x_0 to the vertex set X of a well shaped diagram $\mathcal{G} = (X, E, V)$ of Ω, and to augment the edge set E by connecting every boundary vertex to the super node, and to assign large (say infinite) weights to these edges so that they never lower the conductivity of a path. Also, we may put multiple (say infinite) edges between a boundary node and the super node to guarantee that these edges never increase the congestion. It is convenient to associate the region $V_0 = Q \setminus \Omega$ to the super node x_0.

Notation Given a well–shaped diagram $\mathcal{G} = (X, E, V)$ of Ω, the **augmented diagram** is the diagram formed by adjoining a super node to X and the associated edges and volume to E and V.

LEMMA 4.8. *Let $\mathcal{G} = (X, E, V)$ be an augmented well-shaped diagram of $\Omega \subset \Re^d$. Then there exists a path embedding (ϕ, p) of $\mathcal{G}$ into itself of bounded congestion such that the conductivity of each path in the image is bounded below by a multiple of h_{ij}^{d-2}, i.e. for each edge $(i, j) \in E$*

$$\sum_{(m,n)\in p(i,j)} 1/k_{mn} \le C/h_{ij}^{d-2}.$$

Proof. Let us consider a typical edge $\overline{x_i x_j}$ of length h_{ij} and define U to be the neighborhood of $\overline{x_i x_j}$ consisting of points whose distance from $\overline{x_i x_j}$ is no more than $\min(c/2, \theta c)h_{ij}$ where c and θ are the constants guaranteed by properties $A1$ and $A2$ of Theorem 4.4. We first consider the case when U lies entirely within Ω. The Lipschitz hypotheses on ρ guarantee that $ch_{ij} \le \rho(x) \le (C + c/2)h_{ij}$ for all $x \in U$.

Step 1: *The number of cells from V that intersect U is bounded by a constant $\kappa \ge 0$.*
We use a volume argument. If $x \in V_k \cap U$, property A1 shows that $c/C \le \rho(x_k)/\rho(x) \le C/c$. Since $\rho(x)$ is bounded above and below by multiples of h_{ij}, property A2 implies that V_k contains a ball having volume bounded below by $\hat{c}h_{ij}^d$ and the diameter of V_k is bounded by $\hat{C}h_{ij}$. If $\tilde{U}$ is the set of points having distance no more than $\hat{C}h_{ij}$ from $\overline{x_i x_j}$, then $\tilde{U}$ contains all of the cells intersecting U and has volume bounded by a multiple of h_{ij}^d. It follows that the number of cells meeting U is bounded by $|\tilde{U}|/\hat{c}h_{ij}^d$.

Step 2: *There exists a line segment from V_i to V_j in U, parallel to $\overline{x_i x_j}$, that meets Voronoi faces having areas bounded below by a multiple of h_{ij}^{d-1}*
We use an area argument similar in spirit to the previous volume argument. Consider the collection of line segments in U that start in V_i and end in V_j, and are parallel to $\overline{x_i x_j}$. By construction, the cross-sectional area of this collection is bounded below by a multiple of h_{ij}^{d-1}, say $\hat{c}h_{ij}^{d-1}$. Letting δ be the maximal degree of any vertex guaranteed by property A3, the total number of faces that meet U is bounded by $\kappa\delta$. It follows that some path must encounter faces having areas bounded below by $(\hat{c}/\kappa\delta)h_{ij}^{d-1}$ (otherwise every face would be small and their totality wouldn't exhaust the cross section).

We now observe that these conclusions don't change if a Ω is not convex and a portion of U is exterior to Ω. Since the volume of $U \cap \Omega$ is trivially smaller than that of U, the number of cells meeting U only reduces in this case. Similar reasoning holds for the area argument. Note that all of the line segments
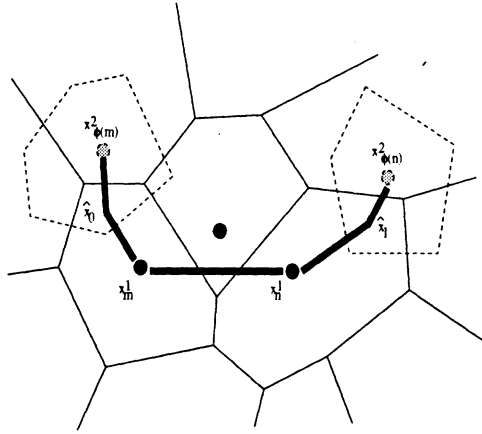
11

FIG. 4. *Path constructed in Theorem 4.9.*

do begin and end in Ω and that we consider all faces on the boundary to have large (infinite) area.

To establish the theorem we let $p(i,j)$ be the path in E formed by connecting the Voronoi centers in the order encountered by a segment in U which only intersects "large" Voronoi faces. This path has length at most κ, and since ρ is bounded above and below by a constant times h_{ij} so too are the lengths of all of edges in $p(i,j)$, which implies a bound the conductivity of the path. Finally, note that an edge in E will only be on a path $p(i,j)$ for vertices x_i and x_j that can be reached along no more than κ edges. Since the degree of each vertex is bounded by the constant δ, the congestion of any edge is less than δ^{κ}. $\square$

THEOREM 4.9. *Let* $\mathcal{G}_1 = (X^{(1)}, E^{(1)}, V^{(1)})$ *be a well-shaped diagram for a cube* Q *containing* Ω *and* $\mathcal{G}_2 = (X^{(2)}, E^{(2)}, V^{(2)})$ *be the augmentation of a well-shaped diagram of* Ω, *each having the same spacing function* ρ. *Then the following construction path embeds* $\mathcal{G}_1$ *into* $\mathcal{G}_2$ *with bounded congestion and dilation:*

1. $\phi(m) = i$ *where* $V_i^{(2)} \in V^{(2)}$ *is a cell intersecting the cell* $V_m^{(1)} \in V^{(1)}$. *(Note that* i *is not uniquely specified as* $V_m^{(1)}$ *can intersect several cells of* $V^{(2)}$*)*

2. *For each edge* $(m,n) \in \mathcal{G}_1$ *consider the three piecewise linear paths:* $S_1 = (x_{\phi(m)}^{(2)}, \hat{x}_0, x_m^{(1)})$, $S_2 = (x_m^{(1)}, x_n^{(1)})$ *and* $S_3 = (x_n^{(1)}, \hat{x}_1, x_{\phi(n)}^{(2)})$ *where* $\hat{x}_0 \in V_m^{(1)} \cap V_{\phi(m)}^{(2)}$ *and* $\hat{x}_1 \in V_n^{(1)} \cap V_{\phi(n)}^{(2)}$ *(see Figure 4). Let* $\ell_1 = \phi(m), \ell_2, \ldots, \ell_{k-1}, \ell_k = \phi(n)$ *index the cells of* $V^{(2)}$ *encountered along the three segments* S_1, S_2, S_3 *in that order. Then* $p(m,n)$ *is the path in* $\mathcal{G}_2$ *formed by the union of the heavily weighted paths from* $x_{\ell_i}^{(2)}$ *to* $x_{\ell_{i+1}}^{(2)}$ *constructed in lemma 4.8.*

Note that this construction is well defined since the super node has the region Q *associated with it, so that every cell* $V_m \in V^{(1)}$ *meets some cell of* $V^{(2)}$, *and paths that leave* Ω *all go to the super node and can reenter anywhere from the super node.*

Proof. Observe that every cell along the path $p(m,n)$ in $V^{(2)}$ intersects either $V_m^{(1)}$, $V_n^{(1)}$ or the edge joining them. Property A1 shows that $ch_{mn} \leq \rho(x) \leq Ch_{mn}$ for every $x \in V_m^{(1)} \cup V_n^{(1)}$, which implies $(c/C^2)h_{mn} \leq \rho(x) \leq C^2/c)h_{mn}$ for $x \in V_{\ell_i}^{(2)}$, $i = 1, 2, \ldots, k$.

An application of the volume argument used in the first step of Lemma 4.8 gives a bound on the length of the path $p(m,n)$. Briefly, the distance from any point in one of the cells $\{V_{\ell_i}^{(2)}\}_{i=1}^{k}$ to S_2 is bounded by a multiple of h_{mn}. This neighborhood of S_2 will have volume bounded by $\hat{C}h_{mn}^d$, and since each of the cells $V_{\ell_i}^{(2)}$ contains a ball having volume bounded below by a multiple of h_{mn}^d, say $\hat{c}h_{mn}$, it follows that there are no more than $\hat{C}/\hat{c}$ such cells. Since the heavily weighted paths constructed in Lemma 4.8 are all of bounded length, the length of $p(m,n)$ is bounded by at most a multiple of $\hat{C}/\hat{c}$.

This immediately leads to bound on the congestion and dilation. Property A3 bounds the degree of any vertex by a constant δ, so the congestion is bounded by the L_{max}^{δ}, where L_{max} is the maximal length of any path. Similarly, the conductivity on each edge is bounded below by a constant of the form $\hat{c}h_{mn}^{d-1}$ and putting L_{max} edges in series doesn't decrease this by more than a factor of $1/L_{max}$. □

COROLLARY 4.10. *Let $\mathcal{G}_1 = (X^{(1)}, E^{(1)}, V^{(1)})$ and $\mathcal{G}_2 = (X^{(1)}, E^{(2)}, V^{(2)})$ be as in the theorem, and suppose that Q is sufficiently large to guarantee that no boundary cell of $V^{(1)}$ meets a boundary cell of $V^{(2)}$. If $\mathcal{G}_1$ satisfies the Poincaré inequality, then so too does $\mathcal{G}_2$*

Proof. Let u be a real valued function on $X^{(2)}$ that vanishes on the boundary (and, in particular on the super node x_0). When constructing the path embedding of $\mathcal{G}_1$ into $\mathcal{G}_2$ given by the theorem, select $\phi(m)$ in step 1 to correspond to the vertex having maximal absolute value of u of the available choices. It follows that

$$|V_i^{(2)}|u_i^2 \leq \sum_m |V_m^{(1)} \cap V_i^{(2)}|u_{\phi(m)}^2,$$

and summing over i gives

$$u^T M^{(2)} u = \sum_i |V_i^{(2)}|u_i^2 \leq \sum_m |V_m^{(1)}|u_{\phi(m)}^2 = (u \circ \phi)^T M^{(1)} (u \circ \phi).$$

Since all boundary vertices of $X^{(1)}$ are mapped by ϕ to the super node $x_0^{(2)}$ it follows that $u \circ \phi : X^{(1)} \longrightarrow \Re$ vanishes on the boundary vertices, and since $\mathcal{G}_1$ satisfies a Poincaré inequality we have

$$u^T M^{(2)} u \leq (u \circ \phi)^T M^{(1)} (u \circ \phi) \leq C(u \circ \phi)^T K^{(1)} (u \circ \phi)$$

and the result follows upon application of Lemma 4.7. □

4.3. Construction of a Graph Satisfying a Poincaré Inequality. In order to apply the results of the previous section to establish a Poincaré inequality for bounded well-shaped diagrams it is necessary to exhibit an instance of a canonical mesh satisfying a Poincaré inequality. We let $\rho : Q \rightarrow \Re^+$ be a specified Lipschitz spacing function, fixed during this discussion, and Q a cube in $\Re^d$.

Figure 5 exhibits the oct–tree construction for a cononical mesh, and the balanceing step is illustrated in Figure 6. The oct–tree construction is well known, and the following lemma shows that our particular contruction generates a well shaped diagram with spacing function ρ.

LEMMA 4.11. *The oct-tree diagram generated by the algorithm of Figure 5 is a well-shaped diagram with spacing function ρ.*

Proof. Properties A3 and A4 follow immediatly from the oct-tree construction. For properties A1 and A2, we only have to show the existance of constants c, $C > 0$ such that each cube Q in the balanced oct-tree generated by the algorithm of Figure 5 satisfies

$$c\ell(Q) \leq \rho(x) \leq C\ell(Q), \qquad x \in Q.$$

Let Q_c be a leaf cube at the end of step 1(b), and let Q be its parent cube. Since Q was divided there is some point $x \in Q$ such that $\rho(x) \leq \ell(Q)$, and since Q_c was not divided, $\ell(Q_c) = \ell(Q)/2 < \rho(y)$ for all $y \in Q_c$. The distance between x and y is bounded by $|x - y| \leq \sqrt{d}\ell(Q)$, and since ρ is α-Lipschitz, $\rho(y) \leq \rho(x) + \alpha\sqrt{d}\ell(Q)$. In summary, by the end of step 1(b),

$$\ell(Q_c) \leq \rho(y) \leq 2(\alpha\sqrt{d} + 1)\ell(Q_c) \qquad y \in Q_c$$

13

```
Algorithm:  Canonical Mesh Construction

Input:   ρ, a spacing function.

Output:  A diargram 𝒢 = (X, E, V).

Method:


   1. Construct a balanced oct-tree:
      (a) Let Q be a cube containing Ω.
      (b) If ℓ_Q denotes the side length of a cube Q, while ℓ_Q > min_Q ρ for any
          cube, Q, sub-divide Q into 2^d cubes.
      (c) While there is a cube Q shareing a (d − 1) face with cube Q̂ having
          ℓ_Q > 2ℓ_Q̂, sub-divide Q.
   2. Assignment of the diagram 𝒢 = (X, E, V).
      (a) The vertices, X, of 𝒢 will be idexed by the cubes of the partition,
          and the cells, V, are the associated cubes.
      (b) 𝒢 has an edge between two verticies x_i and x_j if and only
          if their associated cubes share a d − 1 face, and in this instance the
          edge weight is k_{ij} = min(ℓ_i^{d−2}, ℓ_j^{d−2}), where ℓ_i is the side length of the
          cube Q_i.
      (c) The ''mass'' M_i associated with a particular cell is the volume of
          the associated cube.
```

FIG. 5. *Constructing a canonical mesh.*

We now show there are constants c and C such that after the balancing step 1(c) of the algorithm: $c\ell(Q) \le \rho(y) \le C\ell(Q)$, for $y \in Q$. Since subdividing a cube doesn't affect the lower bound on ρ, we set $c = 1$. To establish the upper bound we use an induction argument. Our induction hypothesis is that prior to any balancing split, all cubes, Q, satisfy $\rho(y) \le C\ell(Q)$ for all $y \in Q$ (C is explicitly computed below).

We have shown that step 1(b) produces cubes satisfying the inductive assumption provided $C \ge 2(\alpha\sqrt{d} + 1)$, establishing the initial inductive step. Let Q be a cube split during the balancing step, Q_c be one of its children, and $\hat{Q}$ be a neighbor causing the split. It follows that $\ell(\hat{Q}) < \ell(Q)/2$, and if $x \in \hat{Q}$ the induction hypothesis guarantees that $\rho(x) \le C\ell(\hat{Q})$. The distance between $x \in \hat{Q}$ and any $y \in Q$ is bounded by

$$|x - y| \le \sqrt{d}\left(\ell(\hat{Q}) + \ell(Q)\right) \le (3\sqrt{d}/2)\ell(Q).$$

Since ρ is Lipschitz with constant α,

$$
\begin{aligned}
\rho(y) &\le \rho(x) + \alpha(3\sqrt{d}/2)\ell(Q) \\
&\le (C/2)\ell(Q) + \alpha(3\sqrt{d}/2)\ell(Q) \\
&\le \left(C/4 + \alpha 3\sqrt{d}/4\right)\ell(Q_c)
\end{aligned}
$$

Selecting C such that $C/4 + \alpha 3\sqrt{d}/4 \le C$ completes the inductive step. □

The construction below mimics the proof of the Poincaré inequality for the continuous case which proceeds by integrating along a path from the boundary to each point in the domain. In the discrete case these paths must lie in the edge set of our graph and no one path can be used to excess (i.e. the congestion must be controlled, see Definition 4.6). The following is a generalization of path
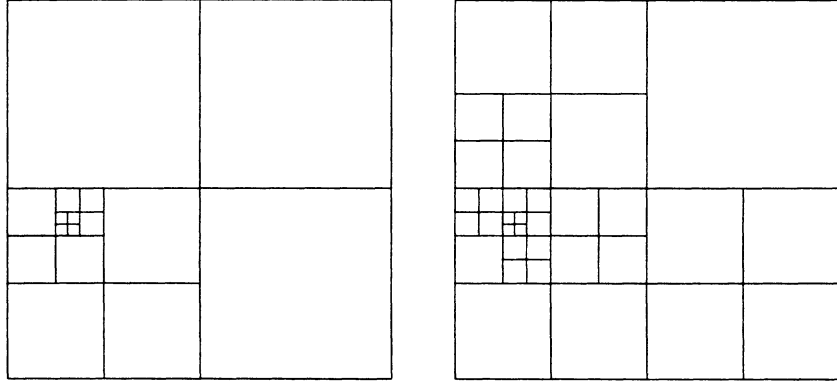
FIG. 6. *Balancing a quad tree.*

embedding of the previous section, where the edges we embed are from each internal vertex to the boundary vertices.

DEFINITION 4.12 (BOUNDARY EMBEDDING). *Let* $\mathcal{G} = (X, E, V)$ *be a graph with edge weights denoted by* k_{ij}. *A* **boundary embedding** *is a collection of graphs* $\{\mathcal{G}_i\}_{x_i \in X}$ *each having the same vertex and edge structure of* $\mathcal{G}$ *and having edge weights* $w_{mn}^{(i)} \geq 0$.

- *The* **congestion** *of the boundary embedding is the maximum over all of the edges* $(m, n) \in E$ *of the sum* $\sum_i w_{mn}^{(i)}$.
- *For* $x_i \in X$ *the* **effective conductivity** *of* $\mathcal{G}_i$ *is the largest constant* $c = c^{(i)}$ *such that*

$$c u_i^2 \leq \sum_{(m,n)} w_{mn}^{(i)} k_{mn} (u_m - u_n)^2$$

for arbitrary nodal values $\{u_m\}$ *vanishing on the boundary.*

The role of these definitions becomes apparent from the following lemma.

LEMMA 4.13. *Let* $\mathcal{G} = (X, E, V)$ *be a well-shaped diagram of* Q *with mass matrix* M *and Laplacian* K. *Let* $\{\mathcal{G}_i\}$ *be a boundary embedding having congestion bounded by* C *and suppose that for each* $\mathcal{G}_i$ *the weighted conductivity is bounded below by* M_i. *Then the Poincaré inequality* $u^T M u \leq C u^T K u$ *holds for all* $u : X \to \Re$ *vanishing on the boundary.*

Proof. The bound on the conductivities guarantees that

$$
\begin{aligned}
u^T M u &= \sum_i M_i u_i^2 \\
&\leq \sum_i \sum_{(m,n)} w_{mn}^{(i)} k_{mn} (u_m - u_n)^2 \\
&\leq \sum_{(m,n)} \left(\sum_i w_{mn}^{(i)} \right) k_{mn} (u_m - u_n)^2 \\
&\leq C u^T K u
\end{aligned}
$$

□

We next construct the subgraphs $\mathcal{G}_i$ alluded to in Lemma 4.13. In the balanced oct-tree we define cube Q_i to be **above** cube Q_j if their projections onto the plane $x_d = 0$ have non-zero $(d-1)$ area. The **horizontal faces** of a cube are the two faces having x_d constant. The key geometric fact used below is that if the intersection of the projections of two cubes have non-zero area, then the projection of the

15

smaller cube must lie entirely within the projection of the larger cube (and the projections coincide if the cubes have the same side lengths).

Consider a vertex x_i in $\mathcal{G}$ and define $\mathcal{G}_i$ to have the same vertex and edge sets as $\mathcal{G}$ and assign weights to the edges of $\mathcal{G}_i$ as follows: An edge (m,n) has non-zero weight if and only if it is associated with a horizontal $d-1$ face and if Q_i is above Q_m and above Q_n. Without loss of generality we order the vertices so that $\ell(Q_m) \leq \ell(Q_n)$, and assign the edge weights by

$$w_{mn}^{(i)} = \begin{cases} \ell(Q_i) & \text{if } \ell(Q_i) > \ell(Q_m) \\ (\frac{\ell(Q_i)}{\ell(Q_m)})^{d-1}\ell(Q_i) & \text{otherwise} \end{cases}$$

THEOREM 4.14. *The graph given by the above construction oct-tree construction satisfies a Poincaré inequality.*

Proof. We show that the graphs $\{\mathcal{G}_i\}$ constructed above satisfy the hypotheses of Lemma 4.13.

Step 1: *The congestion is bounded by $2L$ where L is the side length of Q.*
A fixed (vertical) edge (x_m, x_n) in $\mathcal{G}$, it has a non-zero weight $w_{mn}^{(i)}$ if and only if the cube Q_i lies above the cells V_m and V_n. Without loss of generality, assume $\ell(Q_m) \leq \ell(Q_n)$. Let I index all the cells Q_i above Q_m and Q_n. The congestion is then given by

$$\begin{aligned} c_{mn} &= \sum_{i \in I} w_{mn}^{(i)} \\ &= \sum_{i \in I, \ell(Q_i) \geq \ell(Q_m)} w_{mn}^{(i)} + \sum_{i \in I, \ell(Q_i) < \ell(Q_m)} w_{mn}^{(i)} \\ &= \sum_{i \in I, \ell(Q_i) \geq \ell(Q_m)} \ell(Q_i) + \sum_{i \in I, \ell(Q_i) < \ell(Q_m)} \ell(Q_i)^d / \ell(Q_m)^{d-1} \end{aligned}$$

The first summand is bounded by L since the larger cells must be stacked one on top of the other. The second summand is also less than L since the sum gives the volume of the smaller cells above Q_m divided by the cross sectional area of Q_m. $\square$

Step 2: *Let L be side length of Q, then the effective conductivity of $\mathcal{G}_i$ is bounded below by $M_i = |V_i|$.*
Let ℓ be the minimum side length of the cubes below Q_i (which may be $\ell(Q_i)$), and think of the area of the projection of the cube Q_i onto $x_d = 0$ to be divided into squares of length ℓ. The oct-tree construction guarantees that the projection of a cube Q below Q_i with $\ell(Q) \leq \ell(Q_i)$ will be the union of such squares, and if Q is below Q_i and $\ell(Q) \geq \ell(Q_i)$, then the intersection of the projections of Q_i and Q is equal to the projection of Q_i.

For each square S in the projection, consider the path from the boundary to Q_i formed by connecting the cubes below Q_i that meet the cylinder $S \times \Re$. For convenience label the vertices $m_0, m_1, \ldots, m_I$ so that Q_{m_0} is a boundary cube and $Q_i = Q_{m_I}$. Then

$$\begin{aligned} |S|u_i^2 &= |S| \left(\sum_{n=1}^{I}(u_{m_n} - u_{m_{n-1}}) \right)^2 \\ &\leq \sum_{n=1}^{I} h_{m_n m_{n-1}} \sum_{n=1}^{I}(|S|/h_{m_n m_{n-1}})(u_{m_n} - u_{m_{n-1}})^2 \\ &\leq L \sum_{n=1}^{I}(|S|/h_{m_n m_{n-1}})(u_{m_n} - u_{m_{n-1}})^2 \end{aligned}$$

where L is the side length of Q. Multiplying by $\ell(Q_i)$ and summing this inequality over all squares

16

gives

$$M_i u_i^2 \le L \sum_S \sum_{n=1}^{I_s} (\ell(Q_i)|S|/h_{m_n m_{n-1}})(u_{m_n} - u_{m_{n-1}})^2$$

where $h_{m_n m_{n-1}} = \min(\ell(Q_{m_n}), \ell(Q_{m_{n-1}}))$. If we define $A_{m_n m_{n-1}} = \min(h_{m_n m_{n-1}}, \ell(Q_i))^{d-1}$, interchanging the order of summation gives

$$M_i u_i^2 \le L \sum (\ell(Q_i) A_{m_n m_{n-1}}/h_{m_n m_{n-1}})(u_{m_n} - u_{m_{n-1}})^2$$

where the summation is over all of the horizontal faces below Q_i. The weights $w_{mn}^{(i)}$ were chosen to satisfy $w_{mn}^{(i)} k_{mn} = \ell(Q_i) A_{m_n m_{n-1}}/h_{m_n m_{n-1}}$, hence

$$M_i u_i^2 \le L \sum_{(m,n)\in\mathcal{G}_i} w_{mn}^{(i)} k_{mn}(u_m - u_n)^2$$

□

REFERENCES

[1] I. BABUŠKA AND A. K. AZIZ, *On the angle condition in the finite element method*, SIAM Journal on Numerical Analysis, 13 (1976), pp. 214–226.

[2] M. BERN, D. EPPSTEIN, AND J. R. GILBERT, *Provably good mesh generation*, in 31th Annual Symposium on Foundations of Computer Science, 1990, pp. 231–241.

[3] L. CHEW, *Guaranteed-quality triangular meshes*, CS 89-983, Cornell, 1989.

[4] D. DU AND F. HWANG, *Computing in Euclidean Geometry*, Lecture Notes Series on Computing – Volume 1, World Scientific, 1992.

[5] R. H. MACNEAL, *An asymmetrical finite difference network*, Quarterly of Applied Math, 11 (1953), pp. 295–310.

[6] G. L. MILLER, D. TALMOR, S. TENG, AND N. J. WALKINGTON, *A Delaunay based numerical method for three dimensions: generation, formulation and partition*, in Proceedings of the 27th Annual ACM Symposium on Theory of Computing, 1995.

[7] G. L. MILLER, D. TALMOR, S. TENG, N. J. WALKINGTON, AND H. WANG, *Control volume meshes using sphere packing: Generation, refinement and coarsening*, in 5th International Meshing Round Table, '96, 1996, pp. 47–62.

[8] S. A. MITCHELL AND S. A. VAVASIS, *Quality mesh generation in three dimensions*, in Proceedings of the ACM Computational Geometry Conference, 1992, pp. 212–221. Also appeared as Cornell C.S. TR 92-1267.

[9] R. A. NICOLAIDES, *Direct discretization of plannar div-curl problems*, SIAM Journal on Numerical Analysis, 29 (1992), pp. 32–56.

[10] J. RUPPERT, *A new and simple algorithm for quality 2-dimensional mesh generation*, in Third Annual ACM-SIAM Symposium on Discrete Algorithms, 1992, pp. 83–92.